



Published in final edited form as:

*Cell*. 2010 July 23; 142(2): 270–283. doi:10.1016/j.cell.2010.06.007.

## Essential Regulation of Cell Bioenergetics By Constitutive InsP<sub>3</sub> Receptor Ca<sup>2+</sup> Transfer to Mitochondria

César Cárdenas<sup>1</sup>, Russell A. Miller<sup>3</sup>, Ian Smith<sup>4</sup>, Thi Bui<sup>5</sup>, Jordi Molgó<sup>6</sup>, Marioly Müller<sup>1</sup>, Horia Vais<sup>1</sup>, King-Ho Cheung<sup>1</sup>, Jun Yang<sup>1</sup>, Ian Parker<sup>4</sup>, Craig Thompson<sup>5</sup>, Morris Birnbaum<sup>3</sup>, Kenneth R. Hallows<sup>7</sup>, and J. Kevin Foskett<sup>1,2,\*</sup>

<sup>1</sup> Department of Physiology, University of Pennsylvania, Philadelphia, PA 19104

<sup>2</sup> Department of Cell and Developmental Biology, University of Pennsylvania, Philadelphia, PA 19104

<sup>3</sup> Institute for Diabetes, Obesity and Metabolism, University of Pennsylvania, Philadelphia, PA 19104

<sup>4</sup> Department of Neurobiology and Behavior, University of California, Irvine, CA 92697

<sup>5</sup> Abramson Cancer Institute and Department of Cancer Biology, University of Pennsylvania, Philadelphia, PA 19104

<sup>6</sup> CNRS, Institute de Neurobiologie Alfred Fessard, FRC2118, Laboratoire de Neurobiologie Cellulaire et Moléculaire, UPR 3294, CNRS, 91198 Gif-sur-Yvette cedex, France

<sup>7</sup> Department of Medicine, University of Pittsburgh, Pittsburgh, PA 15261

### Abstract

Mechanisms that regulate cellular metabolism are a fundamental requirement of all cells. Most eukaryotic cells rely on aerobic mitochondrial metabolism to generate ATP. Nevertheless, regulation of mitochondrial activity is incompletely understood. Here we identified an unexpected and essential role for constitutive InsP<sub>3</sub>R-mediated Ca<sup>2+</sup> release in maintaining cellular bioenergetics. Macroautophagy provides eukaryotes with an adaptive response to nutrient deprivation that prolongs survival. Constitutive InsP<sub>3</sub>R Ca<sup>2+</sup> signaling is required for macroautophagy suppression in cells in nutrient-replete media. In its absence, cells become metabolically compromised due to diminished mitochondrial Ca<sup>2+</sup> uptake. Mitochondrial uptake of InsP<sub>3</sub>R released Ca<sup>2+</sup> is fundamentally required to provide optimal bioenergetics by providing sufficient reducing equivalents to support oxidative phosphorylation. Absence of this Ca<sup>2+</sup> transfer results in enhanced phosphorylation of pyruvate dehydrogenase and activation of AMPK, which activates pro-survival macroautophagy. Thus, constitutive InsP<sub>3</sub>R Ca<sup>2+</sup> release to mitochondria is an essential cellular process that is required for efficient mitochondrial respiration and maintenance of normal cell bioenergetics.

---

\*Address correspondence to: J. Kevin Foskett, Department of Physiology, B39 Anatomy-Chemistry Bldg/6085, University of Pennsylvania, Philadelphia, PA 19104-6085, Phone: (215)898-1354, Fax: (215) 573-6808, foskett@mail.med.upenn.edu.

**Publisher's Disclaimer:** This is a PDF file of an unedited manuscript that has been accepted for publication. As a service to our customers we are providing this early version of the manuscript. The manuscript will undergo copyediting, typesetting, and review of the resulting proof before it is published in its final citable form. Please note that during the production process errors may be discovered which could affect the content, and all legal disclaimers that apply to the journal pertain.

## INTRODUCTION

Metabolism provides energy in a useful form to maintain homeostasis and perform work in all cells. ATP production from substrate oxidation and the release of free energy from its hydrolysis must be balanced and sufficient to support cell metabolic needs, including growth, proliferation, production of metabolites and maintenance of homeostatic processes. Most eukaryotic cells rely on mitochondrial oxidative phosphorylation as the major source of ATP. However, the mechanisms by which mitochondrial respiration and ATP synthesis are controlled in intact cells are still not completely understood. Respiratory control models involving kinetic feedback from the products of ATP hydrolysis, allosteric effects of ATP and  $P_i$ , rates of reducing equivalent delivery to mitochondria,  $O_2$  availability, and various controls over respiratory chain components are involved (Balaban, 1990; Brown, 1992; Huttemann et al., 2008). Nevertheless, neither the factors that exert primary control of oxidative phosphorylation and ATP production in the intact cell, nor the signal transduction mechanisms that support the steady state balance of ATP production and utilization, are well understood (Balaban, 1990).

Normal respiration can be altered in several pathological situations (Smeitink et al., 2006; Wallace, 2005), including cancer (Vander Heiden et al., 2009), insufficient nutrient availability, ischemia, injury and exposure to metabolic inhibitors (Huttemann et al., 2008), neurodegenerative (Mattson et al., 2008) and cardiovascular (Gustafsson and Gottlieb, 2008) diseases, and aging (Balaban et al., 2005). In response to decreased cellular ATP, cells employ a variety of pathways to restore homeostasis, including activation of AMP kinase (AMPK) (Hardie, 2007). AMPK phosphorylates substrates to limit anabolic pathways that consume ATP and to activate catabolic pathways to generate substrates to support oxidative phosphorylation (Hardie, 2007). Another mechanism involves activation of macroautophagy (autophagy), a degradation pathway involving delivery of cytoplasmic constituents by double-membrane autophagosomes (AV) that fuse with lysosomal membranes (Klionsky, 2007). Under metabolic stress, pro-survival autophagy is induced, promoting recycling of metabolites to meet metabolic demands, through synthesis of new macromolecules or by their oxidation in mitochondria to maintain ATP levels (Levine and Kroemer, 2008; Lum et al., 2005). Autophagy also functions in developmental cell death, tumor suppression, immunity and aging, and it has been implicated in neurodegeneration, cardiovascular disease and cancer (Levine and Kroemer, 2008).

Here, we have identified a fundamental cellular metabolic control mechanism involving activity of the endoplasmic reticulum-localized inositol trisphosphate receptor ( $InsP_3R$ )  $Ca^{2+}$  release channel. In the absence of basal constitutive low-level  $Ca^{2+}$  signaling by the  $InsP_3R$ , cells become metabolically compromised as a result of diminished  $Ca^{2+}$  uptake by mitochondria. Constitutive mitochondrial  $Ca^{2+}$  uptake of  $InsP_3R$  released  $Ca^{2+}$  is fundamentally required to maintain sufficient mitochondrial NADH production to support oxidative phosphorylation in resting cells. Absence of this  $Ca^{2+}$  transfer results in inhibition of pyruvate dehydrogenase and activation of AMPK, which activates pro-survival autophagy by an mTOR-independent mechanism. These results reveal a here-to-fore unexpected and fundamentally essential role for constitutive low-level  $InsP_3R$   $Ca^{2+}$  release to mitochondria to maintain viable levels of oxidative phosphorylation.

## RESULTS

### The $InsP_3R$ is Required to Inhibit Constitutive Autophagy in Normal Conditions

Chicken DT40 B lymphocytes with all three  $InsP_3R$  isoforms genetically deleted (DT40-KO) is a uniquely  $InsP_3R$ -null cell line (Sugawara et al., 1997). Despite lack of  $InsP_3R$ , DT40-KO cells proliferate indefinitely in normal culture conditions. Transmission electron

microscopy (TEM) revealed a significantly high percentage of KO cells with autophagosomes (AV) ( $36 \pm 2\%$ ) compared with InsP<sub>3</sub>R-expressing WT cells ( $11 \pm 1\%$ ; Figure 1B). Elevated autophagy in KO cells in normal growth conditions was also detected by quantitative measurements of the autophagy marker LC3-II (Klionsky et al., 2008) (Figure 1A). In addition, presence of LC3-GFP puncta associated with early AV formation (Klionsky et al., 2008) was higher in KO ( $18 \pm 4\%$ ) vs WT ( $5 \pm 1\%$ ) cells (Figure 1C). These results suggest that absence of InsP<sub>3</sub>R in DT40-KO cells increases constitutive levels of autophagy. Autophagy was not previously observed in DT40-KO cells (Vicencio et al., 2009), but knockdown of InsP<sub>3</sub>R or its pharmacological inhibition also induces autophagy (Criollo et al., 2007)(and below).

Autophagy in KO cells was not associated with induction of the unfolded protein response (not shown). Lower level of autophagy observed in InsP<sub>3</sub>R-expressing WT cells was not due to intrinsic defects in autophagy, since serum starvation or leucine deprivation induced comparable autophagy in WT and KO cells (Figures S1A–D). Furthermore, mTOR inhibition by rapamycin strongly increased LC3-II levels, whereas 3-methyladenine (3MA), an inhibitor of class III PI-3 kinase involved in AV formation (Levine and Kroemer, 2008), inhibited LC3-II formation, in both lines (Figure S1E). Inhibition of lysosomal proteases enhanced LC3-II in both lines, especially in KO cells (Figures S1F and S1G), indicating that elevated autophagy in KO cells is due primarily to enhanced AV formation.

The specific InsP<sub>3</sub>R inhibitor xestospongine B (XeB) (Jaimovich et al., 2005) increased LC3-II only in WT cells (Figure 2A). XeB increased AV by  $22 \pm 1\%$  (LC3-GFP puncta; Figure S2A) to  $42 \pm 2\%$  (TEM; Figure 2B) in WT cells, whereas KO cells were unaffected. Reduction of InsP<sub>3</sub> production by inhibition of phospholipase C (PLC, by  $5 \mu\text{M}$  U73122) or inositol monophosphatase (IMPase, by  $50 \mu\text{M}$  L-690,488) strongly enhanced LC3-II in WT cells whereas it was without effect on autophagy already present in KO cells (Figure S2B and S2C). XeB also strongly enhanced LC3-II levels and puncta in primary rat pulmonary smooth muscle cells and hepatocytes, and the human breast cancer cell line MCF-7 (Figures S3A–C, S3G and S3H), indicating that autophagy suppression by InsP<sub>3</sub>R activity is a general phenomenon operative in many cell types.

### Functional InsP<sub>3</sub>R Restores Nutrient-Dependent Suppression of Autophagy in KO Cells

Stable expression of InsP<sub>3</sub>R-3 (Figure S2D) completely rescued elevated autophagy in KO cells, measured as either LC3-II content (Figures 2D and S2E) or AV visualization (not shown). To determine if its Ca<sup>2+</sup> channel function was required, we examined cells expressing InsP<sub>3</sub>R-3 containing Thr at position 2591 replaced with Ala (T2591A). T2591A-InsP<sub>3</sub>R-3 expresses at normal levels (Figure S2D), but lacks ion channel activity as a result of a defective channel gate (Foskett, unpublished studies). In contrast to InsP<sub>3</sub>R-3, T2591A-InsP<sub>3</sub>R-3 did not suppress constitutive autophagy (Figure S2E). To determine whether failure to rescue was due specifically to loss of Ca<sup>2+</sup> release activity, we examined KO cells expressing D2550A-InsP<sub>3</sub>R-3 (Figure S2D). This mutant gates normally, whereas it has complete loss of Ca<sup>2+</sup> permeability (Figure 2C). D2550A-InsP<sub>3</sub>R-3 was failed to suppress constitutive autophagy, with a tendency in these cells to have enhanced levels (Figures 2D and 2E). D2550A- and WT-InsP<sub>3</sub>R-3 bound similarly to Beclin-1 (Figure S2L), indicating that disruption of Beclin-1 binding (Vicencio et al., 2009) does not account for autophagy induction by InsP<sub>3</sub>R inhibition. Rather, these results demonstrate that the Ca<sup>2+</sup> release activity of InsP<sub>3</sub>R is necessary for autophagy suppression.

WT and KO DT40 cells were stably transfected with the type 2 ryanodine receptor (RyR2), an InsP<sub>3</sub>R-related Ca<sup>2+</sup> channel expressed in cardiac myocytes, brain neurons, and elsewhere (Fill and Copello, 2002). Caffeine triggered Ca<sup>2+</sup> release (Figure S2F) whereas non-transfected cells failed to respond (not shown). Nevertheless, RyR2 expression was

without effect on constitutive autophagy in KO cells (Figure 2F and S2G). Thus,  $\text{Ca}^{2+}$  release specifically through  $\text{InsP}_3\text{R}$  regulates autophagy in normal nutrient-rich conditions.

### **Requirement for $\text{InsP}_3\text{R}$ $\text{Ca}^{2+}$ Signaling for Autophagy Suppression is Not Due to $\text{Ca}^{2+}$ Dependence of Nutrient Uptake**

Autophagy can be activated by insufficient nutrient uptake (Nicklin et al., 2009). DT40-KO cells reduced glucose in the medium by 67% ( $20 \pm 0.2$  to  $6.6 \pm 0.3$  mM/L) in 24 hr, while WT cells decreased it by 50% ( $20 \pm 0.02$  to  $10 \pm 0.01$  mM/L) (Figure 3A). Similarly, KO cells reduced glutamine by 75% ( $2.37 \pm 0.07$  to  $0.6 \pm 0.01$  mM/L) while WT cells reduced it by 56% ( $2.31 \pm 0.05$  to  $1 \pm 0.07$  mM/L) (Figure 3B). WT and KO cells had similar rates of cytochalasin-B-sensitive deoxyglucose uptake (Figure 3C). Thus, autophagy activation in absence of  $\text{InsP}_3\text{R}$  is not caused by diminished nutrient uptake.

### **Autophagy Activated by Lack of $\text{InsP}_3\text{R}$ Activity is a Cell Survival Mechanism**

Viability was similar in KO ( $90.3 \pm 1.7\%$ ) and WT ( $92.1 \pm 2\%$ ) cells (Figure 3D), suggesting that autophagy in KO cells was not accelerating cell death. To evaluate a role in survival, autophagy was inhibited by pharmacological and genetic means. 3MA reduced viability of KO cells ( $48.3 \pm 7\%$  viable), whereas it had significantly less effect on WT cells ( $78.2 \pm 2.1\%$ ;  $p < 0.001$ ; Figure 3D). Effects on WT cell viability are consistent with an important housekeeping function of low-level basal autophagy (Levine and Kroemer, 2008). Treatment with XeB ( $5 \mu\text{M}$  for 24 hr) killed  $38 \pm 3\%$  of autophagy-deficient primary hepatocytes from Atg5 knockout mice compared with  $1 \pm 0.7\%$  of littermate control cells (Figure 3G). At 48 h,  $65 \pm 2.5\%$  of the Atg5-deficient cells died, compared with  $17 \pm 0.8\%$  of control cells. These results indicate that enhanced autophagy provides a survival mechanism. Consistent with this, when cells were subjected to acute nutrient deprivation by incubation in Hank's medium (24 hr), DT40-KO cells were resistant to death ( $78.2 \pm 2.2\%$  survival) compared with WT cells ( $36.2 \pm 6\%$  survival) (Figure 3E), and this difference was suppressed by 3MA (Figure 3F). When both lines were returned to normal growth medium after 24 hrs in Hank's, KO cells recovered more rapidly than WT cells (Figure 3H). Thus, autophagy is activated in  $\text{InsP}_3\text{R}$ -KO cells as a pro-survival mechanism, and its chronic activation enables them to respond more rapidly and efficiently to nutrient stress, promoting their tolerance and rapid recovery when conditions improve.

### **AMPK Activity is Enhanced by Absence of $\text{InsP}_3\text{R}$ Activity**

Autophagy is activated as a survival mechanism in response to metabolic stress associated with insufficient growth factor stimulation or nutrient availability (Lum et al., 2005). An important mediator of this response is AMPK, a critical metabolic sensor (Hardie, 2007). Although DT40-KO cells did not lack growth factors or nutrients, they nevertheless display enhanced or similar nutrient uptake at the same time they depend on autophagy as a survival mechanism. We therefore examined the role of AMPK, by quantifying phosphorylation of the catalytic  $\alpha$ -subunit. Notably, KO cells had constitutively phosphorylated AMPK (P-AMPK) nearly two-fold greater than in WT cells (Figure 4A). In agreement, phosphorylation of acetyl CoA carboxylase, an AMPK substrate, was also increased in KO cells (data not shown). Enhanced AMPK activity was caused by lack of  $\text{InsP}_3\text{R}$ , because XeB, U73122 or L-690,488 elevated P-AMPK in WT cells, notably to the same levels as in KO cells (Figures 4B, S2H and S2I). Enhanced P-AMPK by XeB was also observed in primary smooth muscle cells and hepatocytes as well as in MCF-7 cells (Figure S3D–S3F). Importantly, treatment of hepatocytes with XeB increased AMP levels and the AMP:ATP ratio (Figure 4J). Elevated P-AMPK in KO cells was reduced to WT levels by expression of  $\text{InsP}_3\text{R}$ -3, but not by expression of  $\text{Ca}^{2+}$  impermeable D2550A- $\text{InsP}_3\text{R}$ -3 (Figure 4C) or RyR-2 (Figure 4D). Thus, both pro-survival autophagy and AMPK activity are upregulated by absence of  $\text{InsP}_3\text{R}$   $\text{Ca}^{2+}$  release activity.

## AMPK, but not mTOR, is Required for Enhanced Autophagy Induced by Absence of InsP<sub>3</sub>R Activity

Enhanced AMPK activity can induce autophagy by inhibition of mTOR (Kimball, 2006). Nevertheless, mTOR phosphorylation was similar in DT40-KO and WT cells (Figure 4E). Furthermore, XeB did not affect P-mTOR in WT cells (Figure 4E), in contrast to its effects on autophagy and P-AMPK. Similarly, phosphorylation of 4E-BP1 or p70<sup>S6K</sup>, two mTOR substrates, were similar in KO and WT cells, and unchanged in WT cells exposed to XeB (Figures 4F and 4G). In contrast, P-p70<sup>S6K</sup> was reduced by starvation or rapamycin (Figure S2J), confirming that mTOR activity is normal in these cells. Thus, autophagy induced by lack of InsP<sub>3</sub>R activity correlates with enhanced AMPK activity, but the mTOR pathway does not appear to be involved.

To determine if AMPK nevertheless links lack of InsP<sub>3</sub>R Ca<sup>2+</sup> release to autophagy activation, we employed pharmacological and genetic approaches. Treatment with the AMPK inhibitor compound C reduced P-AMPK (Figure 4I) and LC3-II (Figure 4H) in KO cells. This suggests that AMPK acts upstream and is required for autophagy activation in response to loss of InsP<sub>3</sub>R activity. To confirm this, we used HEK-293 cells stably expressing either a doxycycline (DOX)-inducible dominant-negative  $\alpha$ 1-AMPK (HEK-K45R), WT  $\alpha$ 1-AMPK (HEK-WT) or the empty vector (HEK-EV) (Hallows et al., 2009). Control experiments confirmed that results obtained in the other cell types were recapitulated in HEK cells. Thus, XeB or U73122 each increased P-AMPK (Figures 5B and S4A) and autophagy (Figures 5C, S3I, S3J and S4B) as a result of enhanced autophagic flux (Figure S4C). IMPase inhibitors L-690-488 and L-690-330 also induced P-AMPK and autophagy, with L-690-488, with better cell penetration, having stronger effects (Figures S4D and S4E). P-p70<sup>S6K</sup> was unaffected by XeB (Figure S4G and S4J), indicating that XeB-induced autophagy in HEK cells was mTOR-independent. Leucine deprivation, which induces autophagy by depressing mTOR activity (Meijer, 2008) potentiated effects of XeB (Figure S4H), and XeB was without effect on normal mTOR inhibition by Hank's or rapamycin (Figure S4G), consistent with additivity of mTOR-dependent and InsP<sub>3</sub>R-associated-independent mechanisms. Thus, InsP<sub>3</sub>R Ca<sup>2+</sup> release channel activity is required for mTOR-independent suppression of autophagy in HEK cells.

Over-expression of AMPK in HEK-WT cells (Figure 5A) increased P-AMPK (Figures 5B and S4A) and enhanced LC3-II (Figure 5C, S3I, S3J and S4B). XeB or U73122 induced autophagy and increased P-AMPK in control HEK-EV cells and HEK-WT cells whereas neither compound induced autophagy or P-AMPK in HEK-K45R cells expressing dominant negative AMPK (Figures 5B, 5C, S3I, S3J, S4A and S4B). These results strongly link autophagy induced by loss of InsP<sub>3</sub>R activity to AMPK activation. In agreement, transient siRNA (Figure 5D) or stable-DOX-inducible shRNA (Figure 5G)  $\alpha$ 1-AMPK knockdown blocked XeB-induced autophagy (Figure 5E, 5H, S3I and S3J) and P-AMPK (Figure 5F and 5I). Together, these results demonstrate a strict requirement for activation of AMPK to link inhibition of InsP<sub>3</sub>R-mediated Ca<sup>2+</sup> signaling to induction of autophagy. Accordingly, a prediction is that cells with AMPK inhibited or knocked down require InsP<sub>3</sub>R for survival. In agreement, 14 ± 1 and 28 ± 2% of the HEK-K45R and shRNA cells, respectively, died following 24 h treatment with XeB, compared with only 3–5% of cells expressing WT AMPK or empty vector (Figure S3K).

### Inhibition of Constitutive InsP<sub>3</sub>R Ca<sup>2+</sup> Release Activity Compromises Cell Bioenergetics

Elevated [AMP] and the requirement for AMPK activation to induce pro-survival autophagy in response to loss of InsP<sub>3</sub>R Ca<sup>2+</sup> signaling suggested that cells lacking this pathway have compromised bioenergetics. We speculated that constitutive low-level InsP<sub>3</sub>R Ca<sup>2+</sup> release promotes oxidative phosphorylation by activation of the ATP synthase (Balaban, 2009;

Territo et al., 2000) and/or dehydrogenases to provide reducing equivalents (McCormack et al., 1990). Cells lacking this pathway, as a consequence of  $\text{InsP}_3\text{R}$  deletion or inhibition of its  $\text{Ca}^{2+}$  release activity, have diminished and uncompensated bioenergetics that are sensed by AMPK that activates autophagy. To test this hypothesis, we attempted to bypass this requirement for  $\text{InsP}_3\text{R}$   $\text{Ca}^{2+}$  signaling by enhancing availability of TCA cycle intermediates to increase production of reducing equivalents. Cells were incubated with membrane permeable methyl-pyruvate (MP) that is oxidized to provide reducing equivalents (NADH) to drive oxidative phosphorylation and ATP production (Lum et al., 2005). Strikingly, MP completely blocked autophagy and it reduced elevated P-AMPK in DT40-KO cells (Figures 5J and 5K) and in XeB-treated HEK cells (Figures 5L and 5M).

To directly evaluate mitochondrial function, cell  $\text{O}_2$  consumption rates (OCR) were measured. Of note, basal OCR was lower by 60% in  $\text{InsP}_3\text{R}$ -KO cells compared with WT cells ( $131 \pm 51$  vs  $44 \pm 18$  pMole  $\text{O}_2/\text{min}/2 \times 10^5$  cells for WT and KO cells respectively; Figure 6A and B). Maximal OCR was also highly reduced in KO cells ( $231 \pm 48$  vs  $614 \pm 63$  pMole  $\text{O}_2/\text{min}/2 \times 10^5$  for KO and WT cells, respectively; Figure 6A and B). Reduced oxidative phosphorylation observed in KO cells was not associated with altered numbers of mitochondria, as evidenced by levels of the mitochondrial marker COX (Figure S2K) and TEM analysis (not shown). These results suggest that oxidative phosphorylation is constitutively compromised in the absence of  $\text{InsP}_3\text{R}$  activity. In contrast, lactate production was enhanced in the KO cells (Figure 6O). To confirm that the observed mitochondrial impairment in KO cells was caused by absence of  $\text{InsP}_3\text{R}$ , OCR was measured in XeB-treated WT and KO cells. XeB dramatically reduced both basal and maximal OCR in WT cells, whereas KO cells were unaffected (Figure 6C). Similar observations were made in HEK cells. Basal OCR was reduced by 57% from  $304 \pm 11$  to  $130 \pm 18$  pMole  $\text{O}_2/\text{min}/8 \times 10^4$  cells by XeB, and maximum OCR was reduced 54% from  $657 \pm 18$  to  $297 \pm 70$  pMole  $\text{O}_2/\text{min}/8 \times 10^4$  cells (Figure 6D). Inhibited OCR was rescued by the  $\text{Ca}^{2+}$  ionophore ionomycin (100 nM; Figure 6E) confirming that availability of  $\text{Ca}^{2+}$  was specifically limiting for normal oxidative phosphorylation. The number of mitochondria was unchanged by XeB (Figure S4F). Measurements in primary smooth muscle cells and cultured PC12 cells yielded similar results (data not shown). Together these results strongly suggest that basal  $\text{InsP}_3\text{R}$  activity is necessary to provide  $\text{Ca}^{2+}$  for optimal mitochondrial oxidative phosphorylation. In its absence, mitochondria consume less  $\text{O}_2$ , reflecting a diminished flux through the electron transport chain.

### **Mitochondrial $\text{Ca}^{2+}$ Uptake Mediates the Effects of $\text{InsP}_3\text{R}$ Activity on Bioenergetics, AMPK Activity and Autophagy**

Our results indicate that constitutive  $\text{InsP}_3\text{R}$ -mediated  $\text{Ca}^{2+}$ -release in non-stimulated cells is necessary for optimal mitochondrial performance. Accordingly, we hypothesized that induction of autophagy could be recapitulated in cells with functional  $\text{InsP}_3\text{R}$  by preventing mitochondrial  $\text{Ca}^{2+}$  uptake. Inhibition of mitochondrial  $\text{Ca}^{2+}$  uptake by the specific  $\text{Ca}^{2+}$  uniporter blocker Ru360 significantly increased LC3-II in DT40-WT cells, whereas it had no effect in KO cells (Figure 6G). Ru360 also enhanced P-AMPK specifically in WT cells (Figure 6H). These effects of Ru360 are remarkably similar to those of XeB, suggesting that their targets are in the same biochemical pathway. In agreement, effects of XeB and Ru360 on LC3-II and P-AMPK were not additive in DT40 (Figures 6G and 6H) or HEK (Figures 6I and 6J) cells. Furthermore, MP prevented Ru360-induced AMPK activation and autophagy induction (Figures 6K and 6L), as it did with XeB (Figures 5L and 5M). Similar to  $\text{InsP}_3\text{R}$ -dependent autophagy, Ru360-induced autophagy was mTOR-independent (Figures S4I and S4J). Autophagy induced by Ru360 was associated with impaired mitochondrial bioenergetics. As with XeB, Ru360 decreased basal OCR by over 50% in both DT40-WT cells and HEK cells (Figures 6M and 6N). In contrast, the constitutively lower basal OCR in

DT40-KO cells was unaffected (Figure 6M). Likewise, maximal OCR also was reduced by 50–60% in both WT DT40 and HEK cells (Figure 6M and 6N). Inhibition of OCR by Ru360 was reversed by ionomycin (100 nM; Figure 6F), again confirming that availability of  $\text{Ca}^{2+}$  was specifically limiting for normal oxidative phosphorylation.

### Pyruvate Dehydrogenase Activity Couples Constitutive $\text{InsP}_3\text{R}$ -Mediated $\text{Ca}^{2+}$ Release to Oxidative Phosphorylation

Mitochondrial matrix  $\text{Ca}^{2+}$  can regulate oxidative phosphorylation at several sites, including the  $\text{F}_1\text{F}_0$ -ATPase and several dehydrogenases, including pyruvate dehydrogenase (PDH) (Balaban, 2009; Territo et al., 2000), a major switch that links glycolysis to the tricarboxylic acid cycle by irreversible decarboxylation of pyruvate. Phosphorylation of PDH by pyruvate kinase suppresses its activity whereas dephosphorylation by  $\text{Ca}^{2+}$ -dependent pyruvate phosphatase enhances it (Patel and Korotchikina, 2006). PDH was hyper-phosphorylated in KO DT40 cells (Figure 7A) and in XeB-treated HEK cells (Figure 7B). Importantly, inhibition of PDH kinases in KO cells by dichloroacetic acid (DCA, 2 mM) (Michelakis et al., 2008) reduced PDH phosphorylation (Figure 7C), restored OCR (Figure 7D) and reduced autophagy (Figure 7E) to control levels. These results suggest that mitochondrial respiration is compromised in the absence of  $\text{InsP}_3\text{R}$  function, and implicate insufficient PDH activity as an important component.

### Constitutive $\text{InsP}_3\text{R}$ -Mediated Low-Level $\text{Ca}^{2+}$ Signaling is Present in Cells in Normal Growth Medium

Our results suggest that constitutive  $\text{InsP}_3\text{R}$   $\text{Ca}^{2+}$  release is necessary for ongoing support of optimal mitochondrial function. We speculated that the important  $\text{Ca}^{2+}$  signals are highly localized, stochastic and occur throughout unstimulated cells to ensure ongoing mitochondrial  $\text{Ca}^{2+}$  uptake to support whole-cell respiration. To observe such signals, we turned to human neuroblastoma SH-SY5Y cells because  $\text{Ca}^{2+}$  release associated with single  $\text{InsP}_3\text{R}$  channel openings can be visualized in them (Smith et al., 2009). We first confirmed that autophagy was similarly regulated by  $\text{InsP}_3\text{R}$  in these cells as in the many cell types studied above. RNAi knock-down of  $\text{InsP}_3\text{R}$ -1, the dominant isoform in these cells (Wojcikiewicz and Luo, 1998) by ~80% (Figure 7F), or treatment with XeB, significantly increased LC3-II (Figures 7G and 7I) and P-AMPK (Figure 7H and 7J). Basal and maximal OCR were inhibited by 33% by XeB (Figure 7K). Ru360 induced autophagy and elevated P-AMPK (Figure S5A and S5B). Thus, as in the other cell types examined in this study, SH-SY5Y cells rely on constitutive  $\text{Ca}^{2+}$  transfer from ER to mitochondria, mediated by  $\text{InsP}_3\text{R}$  and the uniporter, to maintain normal cell bioenergetics.

To image the hypothesized constitutive  $\text{Ca}^{2+}$  signals, we employed total internal reflection fluorescence (TIRF) microscopy with high temporal and spatial resolution (Demuro and Parker, 2006). With perfusion in normal medium, 96% of cells showed spontaneous miniature  $\text{Ca}^{2+}$  release events (Figure 7L *bottom trace* and S5D and video S1), likely representing openings of a single or few  $\text{InsP}_3\text{R}$  channels (Smith and Parker, 2009; Smith et al., 2009), at a frequency of  $22.5 \pm 5$  events/cell/min (Figures 7M and S5D), although many cells displayed >40 events/cell/min (not shown). Transfer to Hank's medium suppressed these events (Figure 7L, *upper trace*), with only 58% of cells displaying  $\text{Ca}^{2+}$  release activity with a 10-fold reduced frequency ( $2.9 \pm 0.7$  events/cell/min) (Figure 7M), with the most active cells displaying at most 10 events/cell/min (not shown). Amplitudes of release events were not different in the two conditions (Figure S5C). Treatment of cells in normal medium with XeB had a similar effect: after XeB only 56% of cells displayed spontaneous  $\text{Ca}^{2+}$  release activity with only  $4.6 \pm 1.5$  events/cell/min compared with  $21.5 \pm 2$  events/cell/min observed in untreated cells. The inhibitory effects of XeB were reversible (Figure 7N).

## DISCUSSION

The most significant finding of our studies is that constitutive low-level InsP<sub>3</sub>R-mediated Ca<sup>2+</sup> release is essential for maintenance of optimal cellular bioenergetics under normal basal conditions. In all of several cell types examined, cells become metabolically compromised in the absence of this ongoing Ca<sup>2+</sup> release activity as a result of diminished Ca<sup>2+</sup> uptake by mitochondria. Previous studies have suggested that agonist-induced InsP<sub>3</sub>R Ca<sup>2+</sup> signals can be transmitted to mitochondria where they can enhance mitochondrial function (Rizzuto et al., 1998; Spat et al., 2008). Our studies demonstrate that mitochondrial uptake of InsP<sub>3</sub>R released Ca<sup>2+</sup> is required for basal mitochondrial bioenergetics in the absence of specific agonist stimulation, and it is fundamentally essential for maintenance of normal cellular bioenergetics. This ongoing Ca<sup>2+</sup> transfer from ER to mitochondria maintains optimal mitochondrial bioenergetics by supporting oxidative phosphorylation, at least in part by providing sufficient reducing equivalents. Reduction of this Ca<sup>2+</sup> transfer results in reduced ATP production and activation of AMPK, which promotes autophagy as a pro-survival mechanism even in the presence of sufficient amino acids to maintain cellular mTOR activation (Figure S6). These results reveal a here-to-fore unexpected essential role for constitutive low-level InsP<sub>3</sub>R-mediated Ca<sup>2+</sup> delivery to mitochondria to preserve normal cellular bioenergetics.

### Constitutive InsP<sub>3</sub>R Ca<sup>2+</sup> Release is Required to Inhibit Pro-Survival Autophagy in Normal Conditions

The InsP<sub>3</sub>R has been implicated in mTOR-independent autophagy (Criollo et al., 2007; Sarkar et al., 2005; Vicencio et al., 2009; Williams et al., 2008). Our results identify a molecular mechanism for this regulation that involves AMPK and impaired cellular bioenergetics when InsP<sub>3</sub>R activity is compromised. Inhibition of autophagy by expression of WT but not mutants deficient in Ca<sup>2+</sup> release that nevertheless have similar binding to Beclin-1 demonstrates that InsP<sub>3</sub>R suppresses autophagy by its ability to release Ca<sup>2+</sup> into the cytoplasm. The role of released Ca<sup>2+</sup> was unrelated to a Ca<sup>2+</sup> requirement for nutrient uptake, as this was not diminished, but was rather somewhat enhanced in cells lacking the InsP<sub>3</sub>R. Enhanced nutrient uptake, activation of AMPK and induction of pro-survival autophagy associated with inhibition of InsP<sub>3</sub>R Ca<sup>2+</sup> release are responses normally observed in cells in nutrient deficient conditions. Thus, lack of constitutive InsP<sub>3</sub>R Ca<sup>2+</sup> signaling activates a *bone fide* pro-survival response to bioenergetic stress despite presence of nutrients and growth factors. That autophagy was activated as a pro-survival mechanism was confirmed by responses of autophagy-deficient HEK cells to InsP<sub>3</sub>R inhibition and of DT40 cells to 3MA, which caused significant death of InsP<sub>3</sub>R activity-deficient cells compared with their WT counterparts, and by the toxicity of XeB in autophagy-deficient Atg5 null cells. In addition, InsP<sub>3</sub>R-deficient cells were much more resistant to actual nutrient deprivation than WT cells, and recovered much more quickly when nutrients were re-supplied, all consistent with activation of autophagy in the absence of InsP<sub>3</sub>R Ca<sup>2+</sup> release as a pro-survival strategy.

### Inhibition of Constitutive InsP<sub>3</sub>R Ca<sup>2+</sup> Release Compromises Cell Bioenergetics

Several observations indicate that InsP<sub>3</sub>R Ca<sup>2+</sup> release in normal medium is necessary to support optimal cellular bioenergetics. First, inhibition of InsP<sub>3</sub>R activity or expression resulted in AMPK activation. AMPK is a highly sensitive indicator of cellular energy status, whose activity increases under conditions of metabolic stress that elevate the cytoplasmic AMP:ATP ratio (Hardie, 2007). In agreement, inhibition of InsP<sub>3</sub>R increased [AMP] and AMP:ATP. AMPK activation was blocked by MP, consistent with reduced mitochondrial ATP production in cells with diminished InsP<sub>3</sub>R Ca<sup>2+</sup> release activity. This conclusion is also supported by OCR measurements that directly interrogate the rate of electron transfer to



oxygen in complex IV of the electron transport chain. Basal OCR was significantly reduced in cells with InsP<sub>3</sub>R activity diminished, indicating that ATP production was reduced. This was true under short-term conditions, when channel activity was inhibited with XeB, and under chronic conditions, exemplified in DT40-KO cells where no compensatory upregulation of OCR was evident. Rather, enhanced lactate production suggests that increased glycolysis, in addition to autophagy, were compensatory responses to compromised cell bioenergetics.

### Mitochondrial Ca<sup>2+</sup> Uptake Mediates Effects of InsP<sub>3</sub>R Activity on Bioenergetics

Maximal OCR in uncoupled mitochondria was also reduced in cells lacking InsP<sub>3</sub>R activity. Failure of an uncoupler to normalize OCR between cells having or lacking InsP<sub>3</sub>R activity suggests that the mitochondrial deficiency resides in their inability to produce sufficient NADH to maintain electron flow through the respiratory complex. Whether this deficiency also accounts for reduced basal respiration is not as clear. However, PDH became hyperphosphorylated (inactivated) in cells lacking InsP<sub>3</sub>R activity, and reversal of this by inhibition of PDH kinases restored normal oxidative phosphorylation and inhibited constitutive autophagy. These results are most consistent with InsP<sub>3</sub>R activity being linked to regulation of cell bioenergetics through constitutive Ca<sup>2+</sup> dependent regulation of the PDH phosphatase. PDH, and two other rate-limiting metabolic enzymes,  $\alpha$ -ketoglutarate- and isocitrate-dehydrogenases, are activated by matrix Ca<sup>2+</sup>, generating NADH required for ATP synthesis (McCormack et al., 1990). Ca<sup>2+</sup> permeation into mitochondria is rate-limited at the inner membrane, where uptake occurs through the uniporter channel, driven by the membrane voltage generated by electron transport in normally-respiring mitochondria (Spat et al., 2008). Ca<sup>2+</sup> uptake by mitochondria *in vitro* occurs over a range of 1–100  $\mu$ M Ca<sup>2+</sup> (Spat et al., 2008; Szabadkai and Duchen, 2008). Nevertheless, InsP<sub>3</sub>-linked agonists that generate sub- $\mu$ M global [Ca<sup>2+</sup>]<sub>i</sub> elevations trigger large increases in mitochondrial matrix [Ca<sup>2+</sup>] (Spat et al., 2008) because of close appositions between mitochondria and ER supported by physical linkages (Csordas et al., 2006; Rizzuto et al., 1998). In these confined spaces, Ca<sup>2+</sup> released through InsP<sub>3</sub>R can reach levels sufficient for permeation through the uniporter (Rizzuto et al., 1998). In our studies, the uniporter inhibitor Ru360 elicited all of the cellular responses observed in cells with diminished InsP<sub>3</sub>R Ca<sup>2+</sup> release. Thus, Ru360 inhibited OCR, activated AMPK and induced autophagy. Ru360 was without effect on cells with InsP<sub>3</sub>R Ca<sup>2+</sup> release compromised, indicating that ER Ca<sup>2+</sup> release and mitochondrial Ca<sup>2+</sup> uptake are in the same pathway that impinges on cell bioenergetics and autophagy. Importantly, the metabolic deficits induced by Ru360, like those induced by disrupted InsP<sub>3</sub>R function, were completely reversed by ionomycin and MP, reinforcing the conclusion that a major defect in cells lacking InsP<sub>3</sub>R activity is insufficient Ca<sup>2+</sup> dependent NADH production to support electron transport.

Whereas the PLC/InsP<sub>3</sub>/Ca<sup>2+</sup> system has been widely considered within the context of agonist stimulation, most studies have used basic salt solutions lacking nutrients and growth factors. The experimental rationale for use of such solutions is obvious, but they are unphysiological and, indeed, similar to those used to induce starvation-mediated autophagy. Cells in their normal milieu are bathed in a variety of factors, some of which impinge on the PLC/InsP<sub>3</sub> system. Low [InsP<sub>3</sub>]<sub>i</sub> likely exist in all cells *in vivo* and can be expected to drive low-level InsP<sub>3</sub>R Ca<sup>2+</sup> release activity. We confirmed this by demonstrating that whereas spontaneous InsP<sub>3</sub>R-mediated Ca<sup>2+</sup> release events are rare in saline buffer, they are quite frequent in cells bathed in medium containing nutrient and growth factors that more closely mimics *in vivo* conditions. These events were transient and highly localized, consistent with stochastic release from one to a few InsP<sub>3</sub>R throughout the cytoplasm (Smith and Parker, 2009; Smith et al., 2009). Optimal production of NADH in mitochondria is achieved by repetitive transient Ca<sup>2+</sup> spikes (Hajnóczky et al., 1995; Jouaville et al., 1999; Robb-Gaspers

et al., 1998; Szabadkai and Duchen, 2008), whereas sustained  $\text{Ca}^{2+}$  release can be associated with mitochondrial  $\text{Ca}^{2+}$  over-load that could activate the mitochondrial transition pore, with possible detrimental consequences including apoptosis and necrosis (Szalai et al., 1999).

In summary, we have identified an essential cellular process that is required for efficient mitochondrial respiration and maintenance of normal cell bioenergetics that involves constitutive  $\text{Ca}^{2+}$  transfer from the ER to mitochondria mediated by the  $\text{InsP}_3\text{R}$ . Because of the fundamental importance of cellular bioenergetics control in normal cellular physiology and pathophysiology, as well as the role of autophagy in diverse human pathologies (Levine and Kroemer, 2008), identification of this process has broad implications.

## EXPERIMENTAL PROCEDURES

### Reagents

Details can be found in Supplemental Experimental Procedures.

### Cell Culture and Transfection

Details can be found in Supplemental Experimental Procedures.

### Detection of Autophagy

**Western blot**—Details can be found in Supplemental Experimental Procedures.

**Electron Microscopy**—Cells were fixed in 2.5% glutaraldehyde in 0.1M cacodylate buffer, postfixed in 2% osmium tetroxide, dehydrated and embedded in Epon, and examined with a high-voltage electron microscope (Philips EM 410). Autophagosomes were identified by classic morphologic features of size  $>0.5 \mu\text{m}$ , presence of a double-limiting membrane, and heterogeneous intraluminal contents (Eskelinen, 2008).

**Confocal Microscopy**—GFP-LC3 expressing cells were fixed with 4% paraformaldehyde and GFP fluorescence was visualized with a Zeiss Axiovert 510 LSM Pascal confocal microscope using a 488 nm laser line.

### Nutrient Uptake

DT40 cells were seeded ( $5 \times 10^4$  cells  $\text{ml}^{-1}$ ) in complete media and cultured in standard conditions ( $37^\circ\text{C}$ , 95%/5% air/ $\text{CO}_2$ ). Media in flasks lacking cells was used to control for nutrient degradation. Media was analyzed by a metabolite analyzer (Novaflex BioProfiles). Cells were counted daily, and nutrient disappearance from the media was normalized to cell number.

### Glucose Transport

DT40 cells were washed with Krebs-BSA buffer, pre-incubated or not with cytochalasin B (10 min) and incubated for 10 min at  $37^\circ\text{C}$  with  $^3\text{H}$ -2-deoxyglucose (DOG = 10 mM). The reaction was stopped by placing it on ice. Samples were spun, decanted, lysed in 1% triton x-100, and cell  $^3\text{H}$  quantified.

### Single Channel $\text{InsP}_3\text{R}$ Recording

$\text{InsP}_3\text{R}$  single channel recording by patch-clamp electrophysiology of isolated DT40 cell nuclei was performed as described (White et al., 2005). Ion selectivity was performed as described (Mak and Foskett, 1994), with reversal potentials corrected for liquid junction potentials.

### Cell Viability

Viability assays were performed as described (Shimizu et al., 2004). Details can be found in Supplemental Experimental Procedures.

### Oxygen Consumption

Oxygen consumption rate (OCR) was measured in at 37°C using an XF24 extracellular analyzer (Seahorse Bioscience). Details can be found in Supplemental Experimental Procedures.

### Calcium Imaging

Details can be found in Supplemental Experimental Procedures.

### Quantification of adenine nucleotides

Nucleotides were extracted from primary hepatocytes using perchloric acid, neutralized, and frozen for subsequent HPLC analysis (Kochanowski et al., 2006). AMP, ADP, and ATP in extracted samples were quantified using ion-pair reverse-phase HPLC, with a C18 RP column, under isocratic elution conditions in 200 mM phosphate, 5 mM tetrabutylammonium phosphate, and 3% acetonitrile.

### Analysis and Statistics

All data summarized as mean  $\pm$  SEM; significance of differences was assessed using unpaired *t*-tests. Differences were accepted as significant at the 95% level ( $p < 0.05$ ).

### Supplementary Material

Refer to Web version on PubMed Central for supplementary material.

### Acknowledgments

We thank Dr. Robert Balaban for helpful discussions. This work was supported by NIH grants GM/DK56328 and MH059937 (J.K.F.), DK075048 (K.R.H.), CA099179 and CA092660 (C.T.), GM48071 (I.P.), and GM065830 (J.K.F. and I.P.). We thank the University of Pennsylvania Institute for Diabetes, Obesity and Metabolism (P30-DK19535) for assistance. C.C. was supported by an award from the American Heart Association. RAM was supported by DK079572.

### References

- Balaban RS. Regulation of oxidative phosphorylation in the mammalian cell. *The American journal of physiology*. 1990; 258:C377–389. [PubMed: 2138418]
- Balaban RS. The role of Ca<sup>2+</sup> signaling in the coordination of mitochondrial ATP production with cardiac work. *Biochimica et biophysica acta*. 2009; 1787:1334–1341. [PubMed: 19481532]
- Balaban RS, Nemoto S, Finkel T. Mitochondria, oxidants, and aging. *Cell*. 2005; 120:483–495. [PubMed: 15734681]
- Brown GC. Control of respiration and ATP synthesis in mammalian mitochondria and cells. *The Biochemical journal*. 1992; 284(Pt 1):1–13. [PubMed: 1599389]
- Criollo A, Maiuri MC, Tasdemir E, Vitale I, Fiebig AA, Andrews D, Molgó J, Diaz J, Lavandero S, Harper F, et al. Regulation of autophagy by the inositol trisphosphate receptor. *Cell Death Differ*. 2007; 14:1029–1039. [PubMed: 17256008]
- Csordas G, Renken C, Varnai P, Walter L, Weaver D, Buttle KF, Balla T, Mannella CA, Hajnoczky G. Structural and functional features and significance of the physical linkage between ER and mitochondria. *J Cell Biol*. 2006; 174:915–921. [PubMed: 16982799]
- Demuro A, Parker I. Imaging single-channel calcium microdomains. *Cell Calcium*. 2006; 40:413–422. [PubMed: 17067668]

- Eskelinen EL. To be or not to be? Examples of incorrect identification of autophagic compartments in conventional transmission electron microscopy of mammalian cells. *Autophagy*. 2008; 4:257–260. [PubMed: 17986849]
- Fill M, Copello JA. Ryanodine receptor calcium release channels. *Physiol Rev*. 2002; 82:893–922. [PubMed: 12270947]
- Gustafsson AB, Gottlieb RA. Heart mitochondria: gates of life and death. *Cardiovascular research*. 2008; 77:334–343. [PubMed: 18006487]
- Hajnoczky G, Robb-Gaspers LD, Seitz MB, Thomas AP. Decoding of cytosolic calcium oscillations in the mitochondria. *Cell*. 1995; 82:415–424. [PubMed: 7634331]
- Hallows KR, Alzamora R, Li H, Gong F, Smolak C, Neumann D, Pastor-Soler NM. AMP-activated protein kinase inhibits alkaline pH- and PKA-induced apical vacuolar H<sup>+</sup>-ATPase accumulation in epididymal clear cells. *American journal of physiology*. 2009; 296:C672–681. [PubMed: 19211918]
- Hardie DG. AMP-activated/SNF1 protein kinases: conserved guardians of cellular energy. *Nat Rev Mol Cell Biol*. 2007; 8:774–785. [PubMed: 17712357]
- Huttemann M, Lee I, Kreipke CW, Petrov T. Suppression of the inducible form of nitric oxide synthase prior to traumatic brain injury improves cytochrome c oxidase activity and normalizes cellular energy levels. *Neuroscience*. 2008; 151:148–154. [PubMed: 18037245]
- Jaimovich E, Mattei C, Liberona JL, Cárdenas C, Estrada M, Barbier J, Debitus C, Laurent D, Molgó J. Xestospongins B, a competitive inhibitor of IP<sub>3</sub>-mediated Ca<sup>2+</sup> signalling in cultured rat myotubes, isolated myonuclei, and neuroblastoma (NG108-15) cells. *FEBS Lett*. 2005; 579:2051–2057. [PubMed: 15811317]
- Jouaville LS, Pinton P, Bastianutto C, Rutter GA, Rizzuto R. Regulation of mitochondrial ATP synthesis by calcium: evidence for a long-term metabolic priming. *Proc Natl Acad Sci U S A*. 1999; 96:13807–13812. [PubMed: 10570154]
- Kimball SR. Interaction between the AMP-activated protein kinase and mTOR signaling pathways. *Med Sci Sports Exerc*. 2006; 38:1958–1964. [PubMed: 17095930]
- Klionsky DJ. Autophagy: from phenomenology to molecular understanding in less than a decade. *Nat Rev Mol Cell Biol*. 2007; 8:931–937. [PubMed: 17712358]
- Klionsky DJ, Abeliovich H, Agostinis P, Agrawal DK, Aliev G, Askew DS, Baba M, Baehrecke EH, Bahr BA, Ballabio A, et al. Guidelines for the use and interpretation of assays for monitoring autophagy in higher eukaryotes. *Autophagy*. 2008; 4:151–175. [PubMed: 18188003]
- Kochanowski N, Blanchard F, Cacan R, Chirat F, Guedon E, Marc A, Goergen JL. Intracellular nucleotide and nucleotide sugar contents of cultured CHO cells determined by a fast, sensitive, and high-resolution ion-pair RP-HPLC. *Anal Biochem*. 2006; 348:243–251. [PubMed: 16325757]
- Levine B, Kroemer G. Autophagy in the pathogenesis of disease. *Cell*. 2008; 132:27–42. [PubMed: 18191218]
- Lum JJ, Bauer DE, Kong M, Harris MH, Li C, Lindsten T, Thompson CB. Growth factor regulation of autophagy and cell survival in the absence of apoptosis. *Cell*. 2005; 120:237–248. [PubMed: 15680329]
- Mak DO, Foskett JK. Single-channel inositol 1,4,5-trisphosphate receptor currents revealed by patch clamp of isolated *Xenopus* oocyte nuclei. *J Biol Chem*. 1994; 269:29375–29378. [PubMed: 7961913]
- Mattson MP, Gleichmann M, Cheng A. Mitochondria in neuroplasticity and neurological disorders. *Neuron*. 2008; 60:748–766. [PubMed: 19081372]
- McCormack JG, Halestrap AP, Denton RM. Role of calcium ions in regulation of mammalian intramitochondrial metabolism. *Physiol Rev*. 1990; 70:391–425. [PubMed: 2157230]
- Meijer AJ. Amino acid regulation of autophagosome formation. *Methods Mol Biol*. 2008; 445:89–109. [PubMed: 18425444]
- Michelakis ED, Webster L, Mackey JR. Dichloroacetate (DCA) as a potential metabolic-targeting therapy for cancer. *British journal of cancer*. 2008; 99:989–994. [PubMed: 18766181]
- Nicklin P, Bergman P, Zhang B, Triantafellow E, Wang H, Nyfeler B, Yang H, Hild M, Kung C, Wilson C, et al. Bidirectional transport of amino acids regulates mTOR and autophagy. *Cell*. 2009; 136:521–534. [PubMed: 19203585]

- Patel MS, Korotchkina LG. Regulation of the pyruvate dehydrogenase complex. *Biochem Soc Trans.* 2006; 34:217–222. [PubMed: 16545080]
- Rizzuto R, Pinton P, Carrington W, Fay FS, Fogarty KE, Lifshitz LM, Tuft RA, Pozzan T. Close contacts with the endoplasmic reticulum as determinants of mitochondrial  $\text{Ca}^{2+}$  responses. *Science (New York, NY)*. 1998; 280:1763–1766.
- Robb-Gaspers LD, Burnett P, Rutter GA, Denton RM, Rizzuto R, Thomas AP. Integrating cytosolic calcium signals into mitochondrial metabolic responses. *Embo J.* 1998; 17:4987–5000. [PubMed: 9724635]
- Sarkar S, Floto RA, Berger Z, Imarisio S, Cordenier A, Pasco M, Cook LJ, Rubinsztein DC. Lithium induces autophagy by inhibiting inositol monophosphatase. *J Cell Biol.* 2005; 170:1101–1111. [PubMed: 16186256]
- Shimizu S, Kanaseki T, Mizushima N, Mizuta T, Arakawa-Kobayashi S, Thompson CB, Tsujimoto Y. Role of Bcl-2 family proteins in a non-apoptotic programmed cell death dependent on autophagy genes. *Nat Cell Biol.* 2004; 6:1221–1228. [PubMed: 15558033]
- Smeitink JA, Zeviani M, Turnbull DM, Jacobs HT. Mitochondrial medicine: a metabolic perspective on the pathology of oxidative phosphorylation disorders. *Cell metabolism.* 2006; 3:9–13. [PubMed: 16399500]
- Smith IF, Parker I. Imaging the quantal substructure of single  $\text{IP}_3\text{R}$  channel activity during  $\text{Ca}^{2+}$  puffs in intact mammalian cells. *Proc Natl Acad Sci U S A.* 2009; 106:6404–6409. [PubMed: 19332787]
- Smith IF, Wiltgen SM, Parker I. Localization of puff sites adjacent to the plasma membrane: functional and spatial characterization of  $\text{Ca}^{2+}$  signaling in SH-SY5Y cells utilizing membrane-permeant caged  $\text{IP}_3$ . *Cell Calcium.* 2009; 45:65–76. [PubMed: 18639334]
- Spat A, Szanda G, Csordas G, Hajnoczky G. High- and low-calcium-dependent mechanisms of mitochondrial calcium signalling. *Cell Calcium.* 2008; 44:51–63. [PubMed: 18242694]
- Sugawara H, Kurosaki M, Takata M, Kurosaki T. Genetic evidence for involvement of type 1, type 2 and type 3 inositol 1,4,5-trisphosphate receptors in signal transduction through the B-cell antigen receptor. *Embo J.* 1997; 16:3078–3088. [PubMed: 9214625]
- Szabadkai G, Duchen MR. Mitochondria: the hub of cellular  $\text{Ca}^{2+}$  signaling. *Physiology (Bethesda, Md.)* 2008; 23:84–94.
- Szalai G, Krishnamurthy R, Hajnoczky G. Apoptosis driven by  $\text{IP}(3)$ -linked mitochondrial calcium signals. *Embo J.* 1999; 18:6349–6361. [PubMed: 10562547]
- Territo PR, Mootha VK, French SA, Balaban RS.  $\text{Ca}^{2+}$  activation of heart mitochondrial oxidative phosphorylation: role of the F(0)/F(1)-ATPase. *American journal of physiology.* 2000; 278:C423–435. [PubMed: 10666039]
- Vander Heiden MG, Cantley LC, Thompson CB. Understanding the Warburg effect: the metabolic requirements of cell proliferation. *Science (New York, NY)*. 2009; 324:1029–1033.
- Vicencio JM, Ortiz C, Criollo A, Jones AW, Kepp O, Galluzzi L, Joza N, Vitale I, Morselli E, Tailler M, et al. The inositol 1,4,5-trisphosphate receptor regulates autophagy through its interaction with Beclin 1. *Cell Death Differ.* 2009; 16:1006–1017. [PubMed: 19325567]
- Wallace DC. Mitochondria and cancer: Warburg addressed. *Cold Spring Harbor symposia on quantitative biology.* 2005; 70:363–374.
- White C, Li C, Yang J, Petrenko NB, Madesh M, Thompson CB, Foscett JK. The endoplasmic reticulum gateway to apoptosis by Bcl-X<sub>L</sub> modulation of the  $\text{InsP}_3\text{R}$ . *Nat Cell Biol.* 2005; 7:1021–1028. [PubMed: 16179951]
- Williams A, Sarkar S, Cuddon P, Ttofi EK, Saiki S, Siddiqi FH, Jahreiss L, Fleming A, Pask D, Goldsmith P, et al. Novel targets for Huntington's disease in an mTOR-independent autophagy pathway. *Nat Chem Biol.* 2008; 4:295–305. [PubMed: 18391949]
- Wojcikiewicz RJ, Luo SG. Differences among type I, II, and III inositol-1,4,5-trisphosphate receptors in ligand-binding affinity influence the sensitivity of calcium stores to inositol-1,4,5-trisphosphate. *Mol Pharmacol.* 1998; 53:656–662. [PubMed: 9547355]

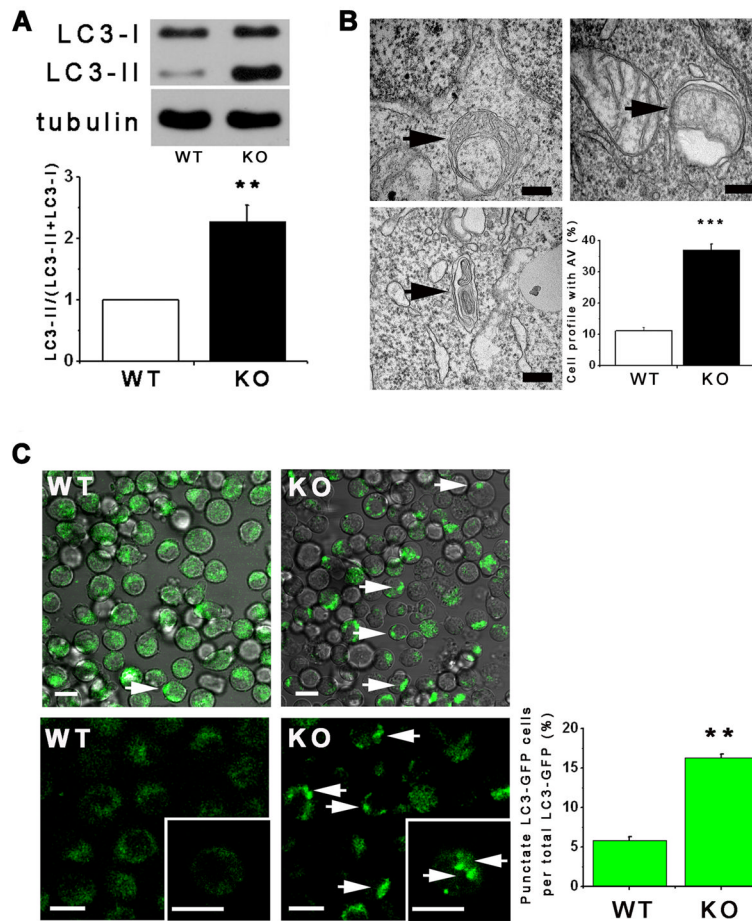


**Figure 1. *InsP<sub>3</sub>R* Deficient Cells Have Elevated Autophagy in Nutrient Rich Conditions**  
 (A) Western blot of LC3 or tubulin in WT and DT40-KO cells (top) and quantification of LC3-II/(LC3-I + LC3-II) (bottom) expressed as fold increase over WT levels (n = 8). (B) TEM of DT40-KO cells showing autophagosomes (AV, arrows), and summary of cell profiles containing AV. 400 profiles counted in 4 experiments. Bars, 50 nm. (C) Confocal images of GFP-LC3 in WT and KO DT40 cells (left and middle panels). Arrows show LC3 puncta (900 cells from 3 experiments with 15 random fields/experiment). \*\*\* p < 0.001, \*\* p < 0.01; Bar, 10  $\mu$ m. See also Figure S1.

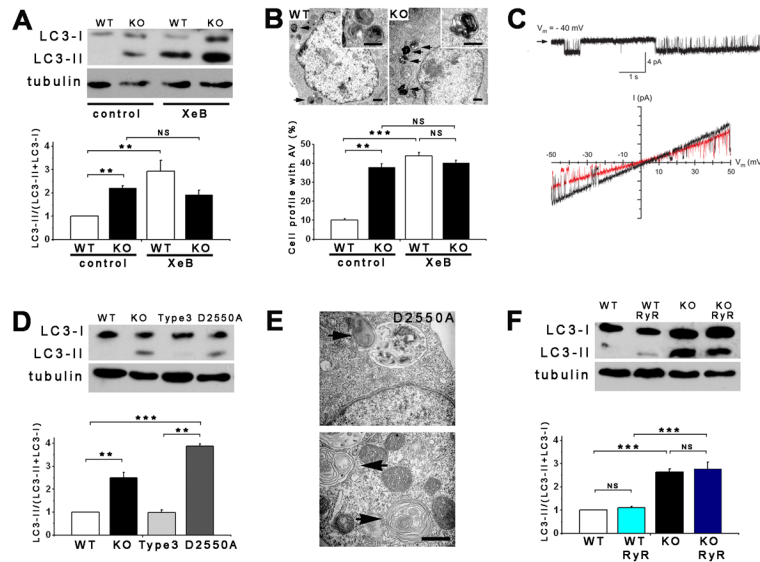


**Figure 2. InsP<sub>3</sub>R Dependence of Autophagy Suppression in Nutrient Rich Conditions** (A) XeB (2  $\mu$ M for 1 h) induces autophagy in WT DT40 cells to levels observed in DT40-KO cells (n = 6). (B) TEM of WT (left) and KO (right) cells showing AV (arrows and insets) after 1 h incubation with 2  $\mu$ M XeB. Bars, 500 nm. Bottom panel summary of 100 cells per experiment counted from 15 fields (n = 3). (C) Current recordings in isolated nuclei from DT40-KO cells expressing D2550A-InsP<sub>3</sub>R-3. Upper: typical gating, arrow represents closed channel current level. Bottom: currents during voltage ramps in control solution (black) and in presence of 10 mM luminal Ca<sup>2+</sup> (red). Lack of normal shift in reversal potential indicates absence of Ca<sup>2+</sup> permeability. (D) Expression of InsP<sub>3</sub>R-3, but not Ca<sup>2+</sup>-impermeable D2550A-InsP<sub>3</sub>R-3, suppresses autophagy in KO cells (n = 3). (E) TEM of AV (arrows) in cells stably-transfected with D2550A-InsP<sub>3</sub>R-3. Bar = 500 nm. (F) RyR-2 expression fails to suppress autophagy in KO cells (n = 3). \*\*\* p < 0.001; \*\* p < 0.01; NS not significant. See also Figures S2, S3 and S4.

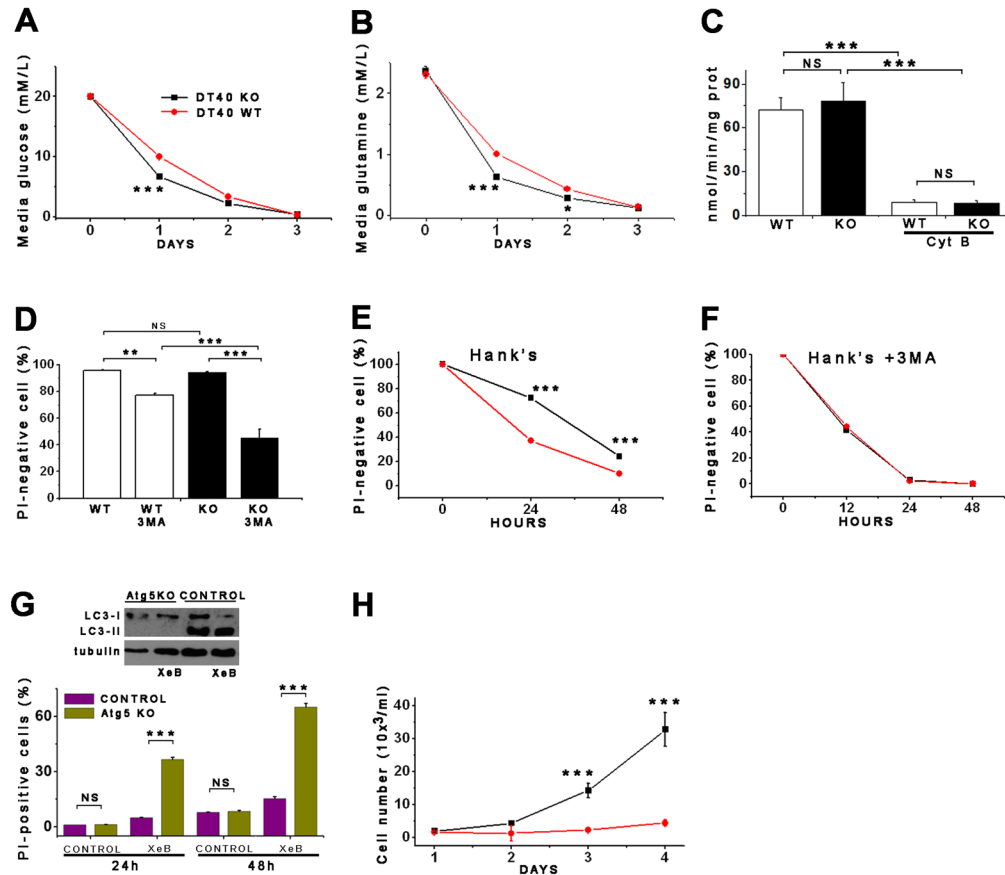


**Figure 3. Lack of  $\text{InsP}_3\text{R Ca}^{2+}$  Release Activity Activates Pro-Survival Mechanisms** (A and B) Glucose (A) and glutamine (B) consumption measured daily in DT40 cells. (C) Cytochalasin B (Cyt B)-sensitive deoxyglucose uptake by WT and KO cells ( $n = 3$ ). (D) Effects of autophagy inhibition by 3MA in nutrient-rich media on viability (PI-negative cells) of WT and KO cells after 24 hr ( $n = 3$ ). (E and F) Survival of WT and KO cells in starvation conditions (Hank's) in absence (E) and presence (F) of 3MA ( $n = 3$ ). (G) Death (PI-positive cells) of Atg5-deficient primary hepatocytes induced by XeB ( $n = 3$ ). (H) Recovery of WT and KO cells after 24 hr starvation. Same number of cells seeded in complete medium ( $n = 3$ ). Error bars shown when bigger than points. \*\*\*  $p < 0.001$ , \*\*  $p < 0.01$ .



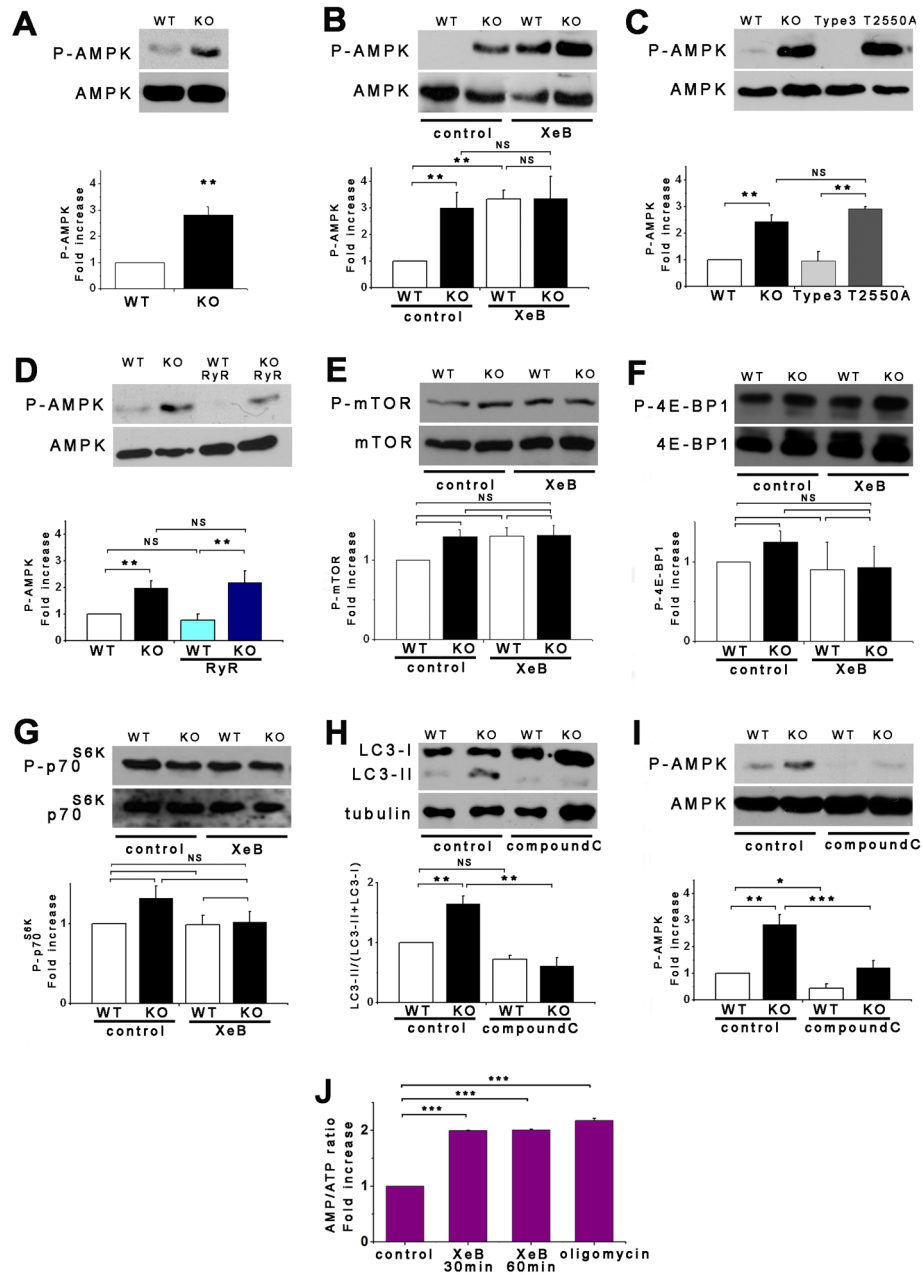


**Figure 4. Pro-Survival Autophagy Induced By Lack of  $\text{InsP}_3\text{R Ca}^{2+}$  Signaling is Associated with Activation of AMPK but not mTOR**

(A) DT40-KO have higher levels of P-AMPK than DT40-WT cells. P-AMPK/AMPK expressed as fold increase over WT levels ( $n = 8$ ). (B) XeB ( $2 \mu\text{M}$  for 1 h) increases P-AMPK in WT cells to levels observed in KO cells ( $n = 6$ ). (C)  $\text{InsP}_3\text{R-3}$  but not  $\text{Ca}^{2+}$ -impermeant D2550A- $\text{InsP}_3\text{R-3}$  reduces high P-AMPK in KO cells to control (WT) levels ( $n = 3$ ). (D) Expression of RyR-2 fails to reduce P-AMPK in KO cells ( $n = 3$ ). (E) mTOR phosphorylation is similar in KO and WT cells and is unaffected by XeB ( $2 \mu\text{M}$  for 2 h). P-mTOR/mTOR levels expressed as fold increase over WT levels ( $n = 5$ ). (F and G) Phosphorylation of mTOR substrates 4E-BP1 and  $\text{p70}^{\text{S6K}}$  in KO and WT cells treated or not with  $2 \mu\text{M}$  XeB for 2h. P-4E-BP1/4E-BP1 or P- $\text{p70}^{\text{S6K}}$ / $\text{p70}^{\text{S6K}}$  levels expressed as fold

increase over WT levels (n = 5). (H and I) AMPK inhibition by compound C (CC; 2.5  $\mu$ M for 1 hr) represses constitutive autophagy and elevated P-AMPK observed in KO cells (n = 5). (J) XeB (2  $\mu$ M, 1 hr) increases AMP/ATP ratio in hepatocytes. AMP/ATP ratio expressed as average fold increase (mean  $\pm$  S.E, n = 3) over untreated conditions. \*p < 0.05, \*\* p < 0.01, \*\*\* p < 0.001, NS not significant. See also Figure S3.

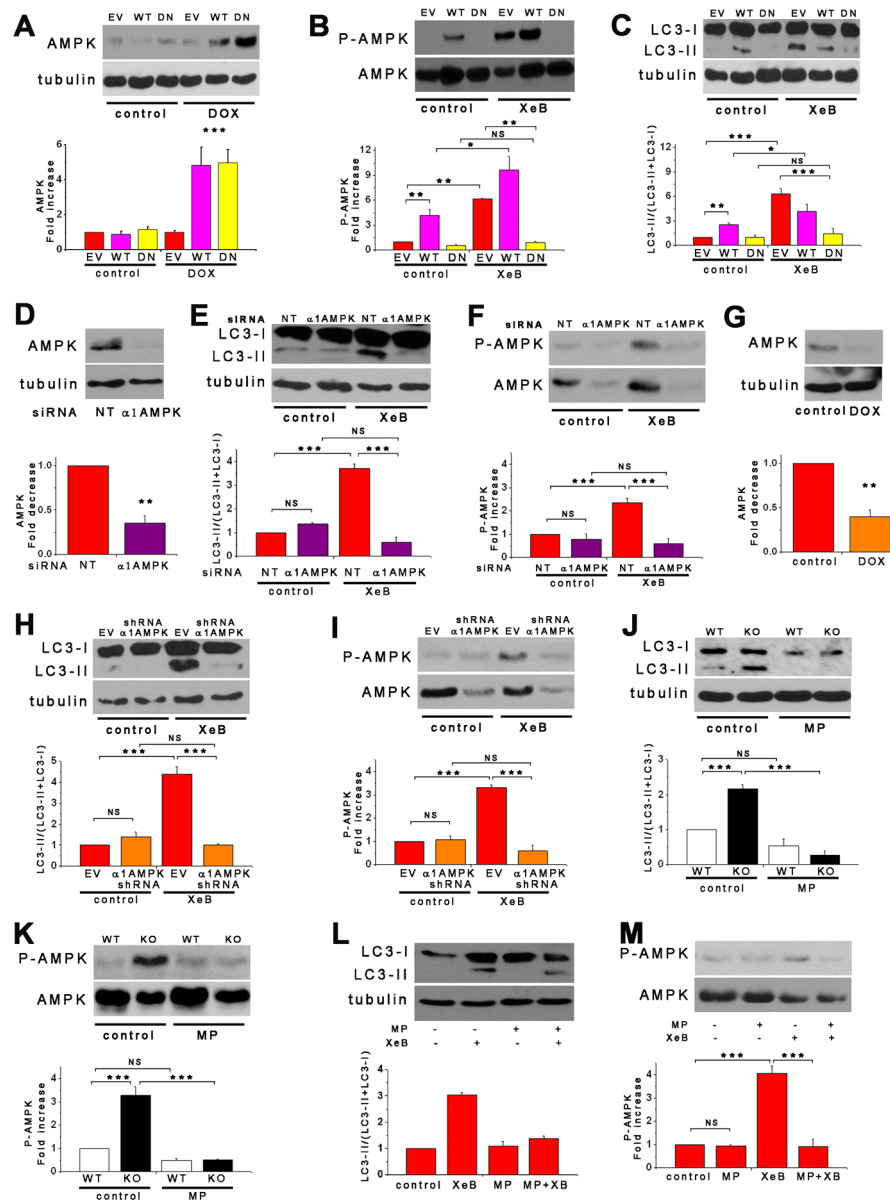


**Figure 5. Pro-Survival Autophagy Induced By Lack of InsP<sub>3</sub>R Ca<sup>2+</sup> Signaling is Mediated by AMPK**

(A)  $\alpha 1$ -AMPK expression in HEK-293 cells stably expressing DOX-inducible WT or dominant negative (DN)  $\alpha 1$ -AMPK in presence or absence of DOX. Cells transfected with empty vector (EV) used as control. AMPK/tubulin expressed as fold increase over basal levels (DOX untreated) (n= 6). (B and C) XeB (2  $\mu$ M for 1 h) failed to trigger either autophagy or AMPK phosphorylation in cells expressing DN-AMPK. Over-expression of WT  $\alpha 1$ -AMPK increased autophagy (n = 6). (D)  $\alpha 1$ -AMPK levels in HEK cells transiently transfected with  $\alpha 1$ -AMPK or irrelevant (NT) siRNA (n = 3). (E and F) XeB fails to induce autophagy or P-AMPK in cells transiently transfected with  $\alpha 1$ -AMPK siRNA (n = 3). (G) HEK-293 cells stably expressing inducible  $\alpha 1$ -AMPK shRNA were exposed to DOX for 72 hr (n = 3). (H and I) XeB fails to induce autophagy and P-AMPK in cells expressing inducible  $\alpha 1$ -AMPK shRNA (n = 3). (J – M) Treatment of DT40-KO (J and K) and HEK-293 (L and M) cells with methyl-pyruvate (MP; 5  $\mu$ M for 1 hr) reduced autophagy and

AMPK hyper-phosphorylation (n = 3). \*p < 0.05, \*\* p < 0.01, \*\*\* p < 0.001, NS, not significant. See also Figures S3 and S4.

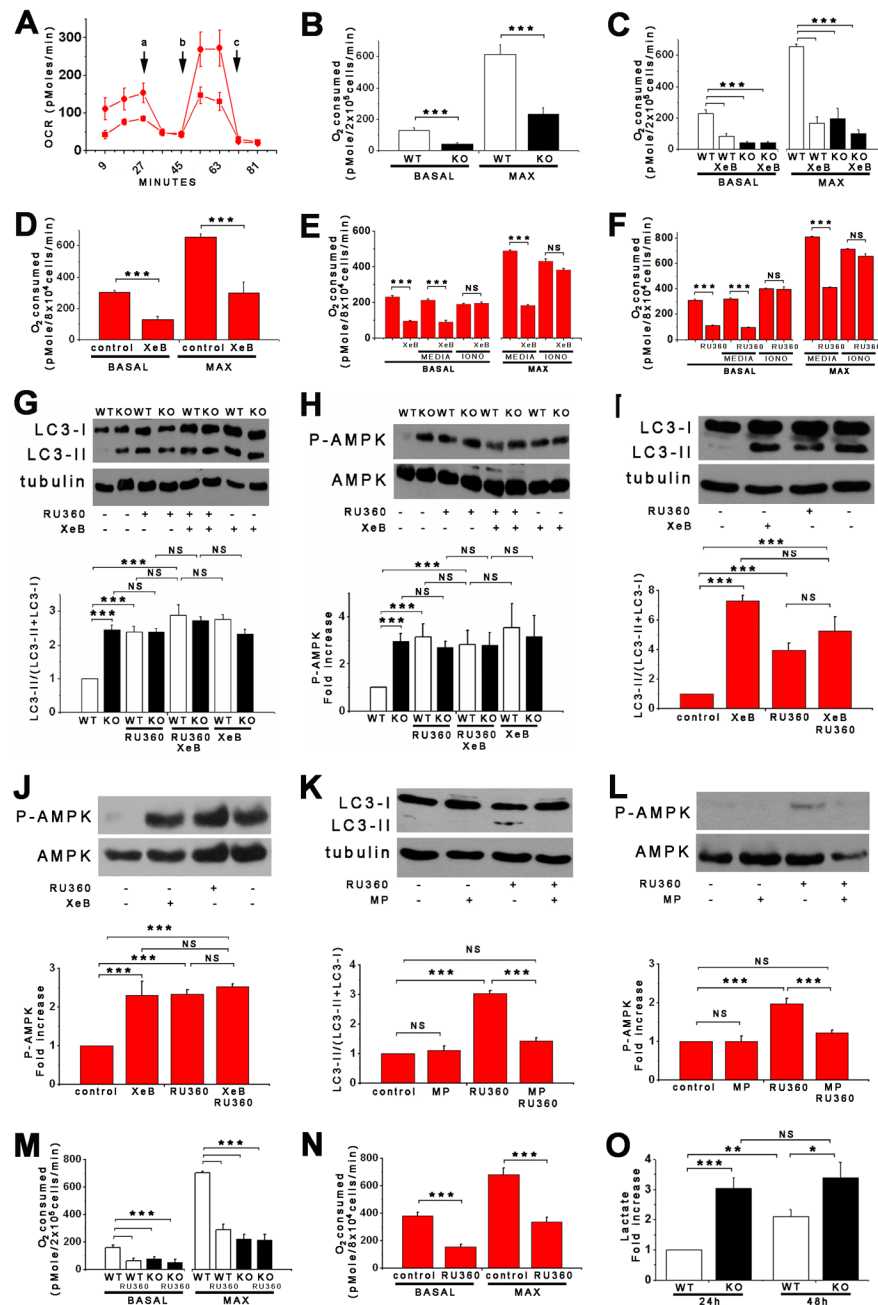


**Figure 6. Lack of  $\text{InsP}_3\text{R Ca}^{2+}$  Signaling and Inhibition of Mitochondrial  $\text{Ca}^{2+}$  Uptake Are in the Same Pathway that Regulates Bioenergetics and Autophagy**

(A) Oxygen consumption rates (OCR) in WT (red) and KO (black) DT40 cells exposed sequentially to (a) oligomycin, (b) FCCP and (c) rotenone plus myzothiazol. (B) Basal and maximal OCR in WT and KO DT40 cells ( $n = 3$ ). (C and D) Basal and maximal OCR in DT40 and HEK-293 cells treated or not with XeB ( $2 \mu\text{M}$  for 1 hr) ( $n = 3$ ). (E – F) The  $\text{Ca}^{2+}$  ionophore ionomycin ( $100 \text{ nM}$ ) reversed inhibitory effects of XeB (E) and Ru360 (F) on OCR. (G – J) Effects of inhibition of mitochondrial  $\text{Ca}^{2+}$  uptake by Ru360 ( $10 \mu\text{M}$  for 1 h) in absence or presence of XeB on autophagy and P-AMPK in DT40 (G and H) and HEK-293 (I and J) cells ( $n = 3$ ). (K and L) Effects of methyl-pyruvate (MP,  $5 \mu\text{M}$ ) on

autophagy and P-AMPK evoked by 10  $\mu$ M Ru360 in HEK-293 cells (n = 3). (M and N) Effects of mitochondrial  $\text{Ca}^{2+}$  uptake inhibition by Ru360 on basal and maximum OCR in DT40 (M) and HEK-293 (N) cells (n = 3). (O) Lactate generation in WT and KO cells after 24h in normal media (n = 3) \*\*\*  $p < 0.001$ , NS not significant. See also Figure S4.

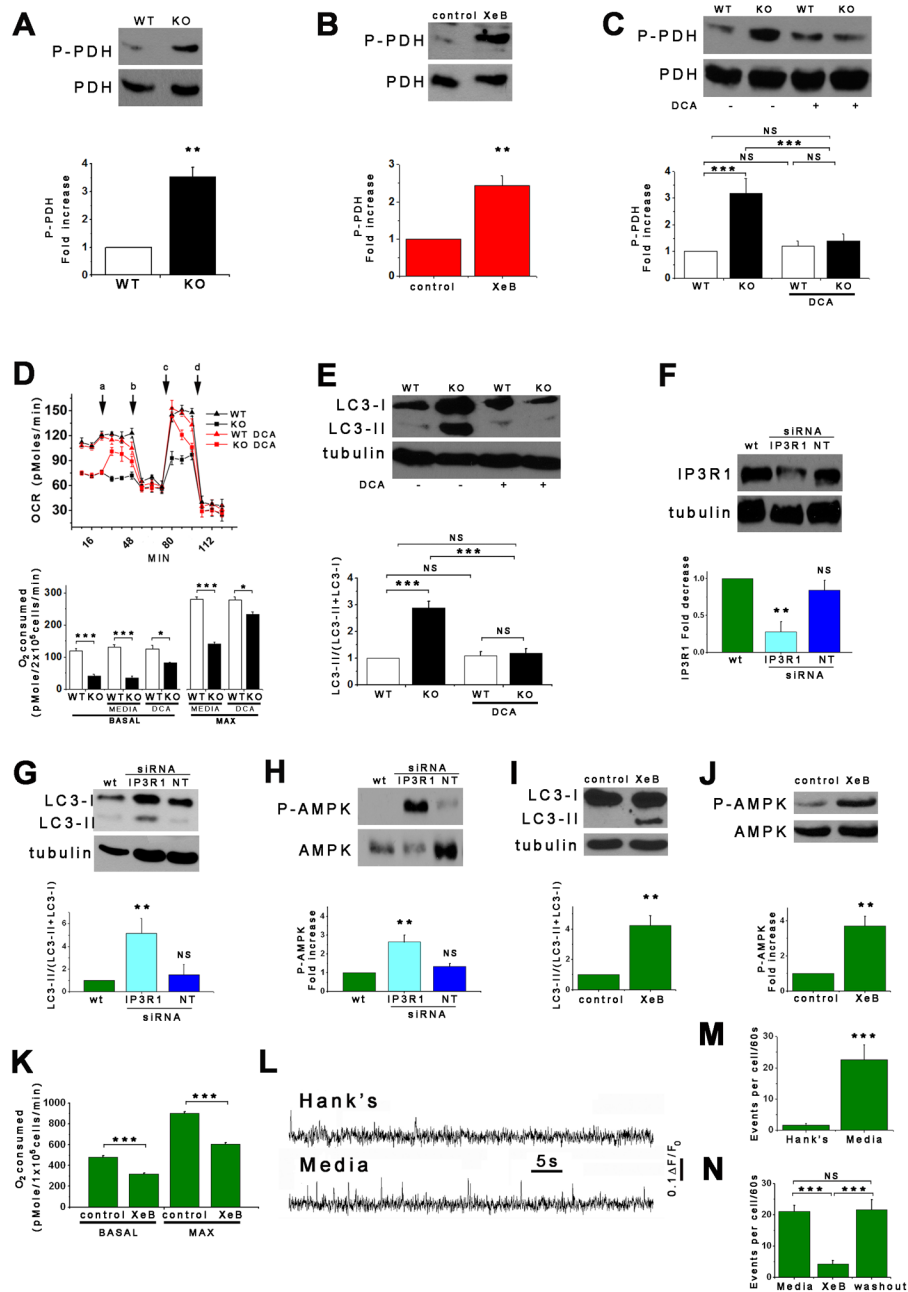


### Figure 7. Normal Growth Medium Supports Constitutive InsP<sub>3</sub>R Ca<sup>2+</sup> Release

(A and B) DT40-KO cells and XeB-treated HEK-293 cells have higher levels of phospho-PDH (n = 3). (C – E) DCA treatment normalizes PDH hyper-phosphorylation (C; 2 mM for 1h), enhances OCR (D; added acutely at “a”) and suppress autophagy (E; 2 mM for 1h) in KO cells to WT levels. (n = 3). (F) Effect of transient transfection (48 h) with specific or irrelevant (NT) siRNA on InsP<sub>3</sub>R-1 expression in SH-SY5Y cells. InsP<sub>3</sub>R-1/tubulin (n = 3) expressed relative to basal levels. (G – J) Effects of InsP<sub>3</sub>R-1 knockdown (G and H) or XeB (10 μM, 1 h) (I and J) on autophagy and P-AMPK in SH-SY5Y cells (n=3). (K) Effects of InsP<sub>3</sub>R-1 knockdown on basal and maximum OCR in SH-SY5Y cells (n=3). (L) Representative fluorescence recordings of Ca<sup>2+</sup> release events in unstimulated SH-SY5Y cells in either Hank’s solution or normal culture media. (M) Quantification of Ca<sup>2+</sup> release

events in SH-SY5Y cells exposed either to Hank's or normal media (n=3 experiments). (N) Effects of XeB (10  $\mu$ M for 30 min) on spontaneous  $\text{Ca}^{2+}$  release events recorded in SH-SY5Y cells in normal media (n=3 experiments). \*\*p < 0.01 \*\*\*p < 0.001. See also Figure S5 and Video S1.